J. Fluid Mech. (1982), *vol.* 121, *pp.* 487–505
Printed in Great Britain

A flow-visualization study of transition in plane Poiseuille flow

By DALE R. CARLSON, SHEILA E. WIDNALL AND MARTIN F. PEETERS

Department of Aeronautics and Astronautics,
Massachusetts Institute of Technology, Cambridge, Massachusetts

(Received 6 July 1981 and in revised form 17 December 1981)

Flow visualization of artificially triggered transition in plane Poiseuille flow in a water channel by means of 10–20 μm diameter titanium-dioxide-coated mica particles revealed some striking features of turbulent spots. Strong oblique waves were observed both at the front of the arrowhead-shaped spot as well as trailing from the rear tips. Both natural and artificially triggered transition were observed to occur for Reynolds numbers slightly greater than 1000, above which the flow became fully turbulent. The front of the spot moves with a convection speed of about two-thirds of the centre-line velocity, while the rear portion moves at about $\frac{1}{3}U_{c1}$. The spot expands into the flow with a spreading half-angle of about 8°. After growing to a size of some 35 times h (the channel depth) at a downstream distance x/h of about 130, the spot began to split into two spots, accompanied by strong wave activity. The spot(s) was followed visually downstream of its origin a distance x/h of about 300. These results indicate that wave propagation and breakdown play a crucial role in transition to turbulence in Poiseuille flow.

1. Introduction

Perhaps one of the most exciting observations made in examining the transition process has been that turbulence first appears in localized regions with a very characteristic shape. These so-called turbulent spots, accompanied by streaky structures, were first observed by Emmons (1951) on a free-surface water table. In the ensuing thirty years since Emmon's observation, the existence of a coherent structure in the final stages of transition for pipe flows, boundary layers and free-surface flows has been well established (Cantwell 1981). However, there seem to be no visual observations or detailed growth measurements for turbulent spots in plane Poiseuille flow.

The goals of the current research effort were to document the structure and behaviour of turbulent spots in a plane Poiseuille flow, to compare the results with similar observations in boundary-layer flows, and to determine whether the observed differences can be understood and lend support to various theoretical models for the structure of turbulence in such flows.

1.1. *Existence of coherent structures*

Prior to the 1950s, turbulence was thought to be a random, statistically describable, process. Emmons' observation of transition in a free-surface flow has resulted in a

view of turbulence as being a collection of rather coherent structures. Following Emmons' (1951) initial observations, there have been a variety of studies of the characteristics of turbulent spots (in both air and water) for both boundary-layer and free-surface flows. With few exceptions, these studies have been of two types: measurements of velocity fields at points in the flow, perhaps using special data-reduction techniques to bring coherence out of chaos; and flow-visualization studies using tracer particles such as smoke, ink, dye or bubbles. In a very fundamental sense, many of our ideas about turbulence come from the fact that most flow-visualization studies have used tracers that followed fluid particles and have presented visual evidence of their behaviour.

The study of the structure of turbulent spots has received considerable attention in recent years. We will therefore not review all past studies but merely highlight those which relate in some way to our study. Early studies were made of the spreading angle and propagation characteristics of spots for both boundary-layer and free-surface flows (Mitchner 1954; Elder 1960; Schubauer & Klebanoff 1956). The orientation of a turbulent spot in a boundary layer was found to be opposite to that in a free-surface flow.

Wygnanski, Sokolov & Friedman (1976) studied the lateral and longitudinal spread of turbulent spots in a Blasius boundary layer and observed a half-angle of spread of about 10°, which varied slightly with Reynolds number. The unsteady laminar flow in the neighbourhood of a spot was measured by Wygnanski, Haritonidis & Kaplan (1979). Wave packets were found to trail the spot at its tips. From calculations of solutions to the Orr–Sommerfeld equation, they concluded that these waves were Tollmien–Schlichting waves. Waves of similar frequency were found inside the turbulent spot, suggesting that the shape, rate of growth, and spreading angle of a spot are related to the coherent wave packet.

Cantwell, Coles & Dimotakis (1978) presented LDV measurements of the structure of the velocity field at the centreline of a spot in a boundary layer and determined the convection speeds of various features of the spot. Of more interest to the present study is the fact that their flow-visualization technique, seeding the flow with flat aluminium flakes, gives visualization similar to that reported here. Discussion of their observations in relation to ours will be given in § 3.

Gad-el-Hak, Blackwelder & Riley (1979), using fluorescent dye illuminated by a narrow sheet of laser light, obtained dramatic pictures of the flow field of a turbulent spot. No strong wave activity was seen directly, but there was some evidence of waves propagating away from the front of the spot. Even with the addition of laser fluorescence, this technique calls attention primarily to the uplift and displacement of dyed particles rather than allowing direct visualization of wave disturbances.

1.2. *Experimental investigations of plane Poiseuille flow*

While there has been considerable theoretical and experimental work done on transition in pipe flows, boundary layers and free-surface flows, there are very few experimental results available for plane Poiseuille flow. This may be attributed to the difficulties associated with constructing an experimental apparatus of large aspect ratio. Many of the early experiments used an aspect ratio that was too low to expect fully developed Poiseuille flow or to avoid side-edge effects, and many experimenters

made little effort to control inlet conditions, flow quality and turbulence level. This becomes evident upon examination of the wide range of transition Reynolds numbers found in the studies. (Reynolds numbers will be based on channel half-depth and centreline velocity.)

Using water as a working fluid, Davies & White (1928) experimentally investigated flow within a rectangular channel of aspect ratio ranging from 170 to 37 and found transitional Reynolds numbers ranging from 266 to 660. However, these results are of limited value since the channel did not have a smooth inlet contraction and the inlet turbulence level was not measured.

Sherlin (1960) investigated flow within a recirculating rectangular water channel of aspect ratio 4 provided with a bellmouth contraction. Disturbances were produced by injecting dye into the fully developed laminar flow, resulting in turbulent 'slugs', a rather poorly defined region of turbulent flow which typically occurs in pipe-flow transition; the slugs grew in the streamwise direction for a Reynolds number above 1265. The 'slugs' of turbulence were observed to have differing front and rear velocities; the ratio $U_{\text{front}}/U_{\text{rear}}$ was found to be a function of the Reynolds number.

Narayanan & Narayana (1967) investigated flow within a rectangular water channel of aspect ratio 12 provided with a two-dimensional contraction zone that was gravity fed by a large reservoir. By injecting dye just downstream of the entry region a turbulent slug was produced and followed downstream for various Reynolds numbers. The Reynolds number at which the rear portion of the slug became more turbulent was defined as the critical transition Reynolds number, found to be 1425. The velocity ratio $U_{\text{rear}}/K_{\text{front}}$ of the turbulent slug was equal to unity up to the critical Reynolds number R_c but decreased for $R > R_c$.

Patel & Head (1969) investigated flow within a rectangular channel of aspect ratio 48, fed with air from a settling box without a contraction zone. Hot-wire surveys showed that turbulent bursts first occurred at a Reynolds number of 1035. They noted that transition in channels was like natural transition in a boundary layer: turbulent bursts and streaks occurred randomly in both spanwise and streamwise directions.

Kao & Park (1970) studied the stability of laminar flow in a rectangular recirculating water channel of aspect ratio 8 with a honeycomb-filled contraction zone. Measurements were made with hot-film anemometers. The neutral stability boundary in the (α, R)-plane was determined from the behaviour of two-dimensional waves generated by a vibrating ribbon. A critical Reynolds number of 2195 was found, below which all small disturbances were damped, and above which there were growing modes.

Karnitz, Potter & Smith (1974) obtained a transition Reynolds number of 5025 in a rectangular channel of aspect ratio 70 connected to a centrifugal blower by a smooth contraction, resulting in a background turbulence level of 0·3 %. They found that sinusoidal waves preceded a turbulent burst, which possessed an essentially plane front as it travelled downstream.

Nishioka, Iida & Ichikawa (1975) studied the stability of plane Poiseuille flow using two-dimensional waves produced by a vibrating ribbon in a channel of aspect ratio 27. Air supplied by an upstream fan passed through a contraction ratio of 27, resulting in a background turbulence level of 0·05 % in the channel. They observed that transition was preceded by intermittent bursts of irregular velocity similar to the turbulent spots found in the transition process for boundary-layer flows. Although laminar flow could be maintained up to a Reynolds number of 8000, nonlinear

subcritical instability occurred when the intensity of subcritical disturbances was above a certain threshold value. This threshold value depended on the Reynolds number and the frequency of the disturbance. Nishioka, Asai & Iida (1980) presented additional results for the secondary breakdown of two-dimensional waves in plane Poiseuille flow created by a vibrating ribbon at Reynolds numbers of about 5000.

In comparing these experimental results, one is struck by the wide variation in transition Reynolds numbers (from 266 to 8000). Although this is not surprising considering the range of experimental techniques and variety of flow apparatus used, it does indicate that transition in plane Poiseuille flow is sensitive to the level of background turbulence. That it occurs over a wide range of Reynolds numbers, extending well below the critical Reynolds number for linear instability (5700), suggests that finite-amplitude effects are important and that it will be less tractable analytically than transition in a boundary layer.

1.3. *Theoretical studies and numerical investigations of the transition process*

Most theoretical studies of the transition process are grounded firmly in the occurrence of linear instability of Tollmien–Schlichting waves. This theory has been remarkably successful at describing the early stages of transition in a boundary layer and the experiments of Schubauer & Skramstad (1948) have established the connection between stability theory and transition. Our understanding of the later stages of transition is not as far advanced.

While wave disturbances play a crucial role in transition, the numerical study of Mack (1967) showed that an arbitrary initial disturbance in a Blasius boundary layer cannot be represented by an infinite set of Tollmien–Schlichting waves (the eigenmodes of the Orr–Sommerfeld equation) with discrete eigenvalues. He found a finite set of discrete eigenvalues and conjectured that there must also exist a continuous spectrum for the Orr–Sommerfeld equation.

Grosch & Salwen (1978) suggested that an arbitrary initial disturbance in a boundary layer must be represented by a finite number of Tollmien–Schlichting modes plus the continuous-spectrum modes (which corresponds to a purely convective motion). Gustavsson (1979) considered the initial-value problem for a Blasius boundary layer and showed analytically that the response to a disturbance consists of discrete waves of the Tollmien–Schlichting type as well as a transient that is related to the continuous spectrum. Gustavsson suggested that interaction between the least-damped Tollmien–Schlichting wave and the convected disturbance of the continuous spectrum could account for the arrowhead shape of a turbulent spot.

Gustavsson (1978) considered the initial-value problem for the development of a wave packet in plane Poiseuille flow for $R > R_c$. His results indicate that waves in a plane Poiseuille flow at these Reynolds numbers will have greater spanwise growth than those in a Blasius boundary layer: a predicted spreading half-angle of 16° (at $R = 6000$) for the former, versus 10° (at $R = 1000$) for the latter. While there is no continuous spectrum in the solution to the Orr–Sommerfeld equation for plane Poiseuille flow, there is a cluster of modes near the wave speed $c_r = \frac{2}{3}$, which may play a role analogous to the continuous spectrum for this flow.

Since transition in plane Poiseuille flow occurs typically at a Reynolds number well below the critical value, calculations using linear theory to predict the behaviour of

wave packets in this flow cannot be expected to provide a complete picture of transition. However, such calculations could indicate what type of strong disturbances in the flow might result from a pointlike perturbation.

Applying the algebraic growth mechanism (resonant forcing of vertical vorticity by damped Tollmien–Schlichting waves) of Gustavsson & Hultgren (1980), Gustavsson (1981) examined the plane Poiseuille case and found eight resonances active at a Reynolds number of about 1000, at which transition to turbulence has been observed by several investigators. How this resonant interaction affects the transition process is as yet unclear, since it leads to algebraic growth only for small times followed by weak exponential decay. However, it does predict the appearance of strong oblique waves in the flow.

Recently, Orszag & Patera (1980) solved the Navier–Stokes equations numerically and found that an initial field of finite-amplitude two-dimensional waves is strongly unstable to infinitesimally small, linear, three-dimensional perturbations. The three-dimensional disturbances to these initial two-dimensional waves were found to grow exponentially in time for Reynolds numbers $R > 1000$.

Thus the various theories for transition in plane Poiseuille flow show a considerable variation in critical Reynolds number and indicate that both finite-amplitude and three-dimensional effects are important.

2. Experimental facility and procedure

2.1. *Experimental facility*

The design goals for the experimental apparatus to investigate transition in plane Poiseuille flow were: (i) to have a channel of large aspect ratio (> 100) and accurate dimensions; (ii) to have an extremely low background turbulence level; and (iii) to develop a straightforward flow-visualization technique.

To achieve a low-turbulence background flow and to provide opportunities for good flow visualization, a blowdown water channel was constructed (figure 1). The flow channel had a depth of 6 mm, a cross-section of 80 cm (aspect ratio 133), and a length of 4·10 m. The final 2·30 m was the test, or observation, section. The channel walls were made of military-grade, craze-resistant, 2·54 cm thick Plexiglas sheet. The channel depth was fixed by the thickness of the side walls. The side walls were made of Plexiglas strips, 6 cm by 6 mm, with a total length of 4·10 m. The channel front and back walls were bolted together on either side of the side strips; neoprene seals at the bolt locations were used to insure watertightness (figure 2*a*).

The channel inlet was connected to a 2·5 m^3 supply tank via a three-dimensional contraction of area ratio 1:100. The supply tank was maintained at a constant head throughout each experimental run by the use of a Mariotte flask (figure 2*b*). The tube in the second reservoir was open to the atmosphere to insure that the pressure in the sealed tanks remained atmospheric at the level of the pipe exit (if the flow rates were not too large). Our measurements indicated that the velocity in the channel remained constant as the level in the reservoirs dropped. This device introduced no noticeable disturbances into the supply tank during an experimental run.

The Reynolds number of any particular experimental run was selected by controlling the position of a wedge-shaped valve at the channel outlet (figure 2*c*). The valve was positioned by a pair of rack-and-pinion gears which were driven by a worm-gear

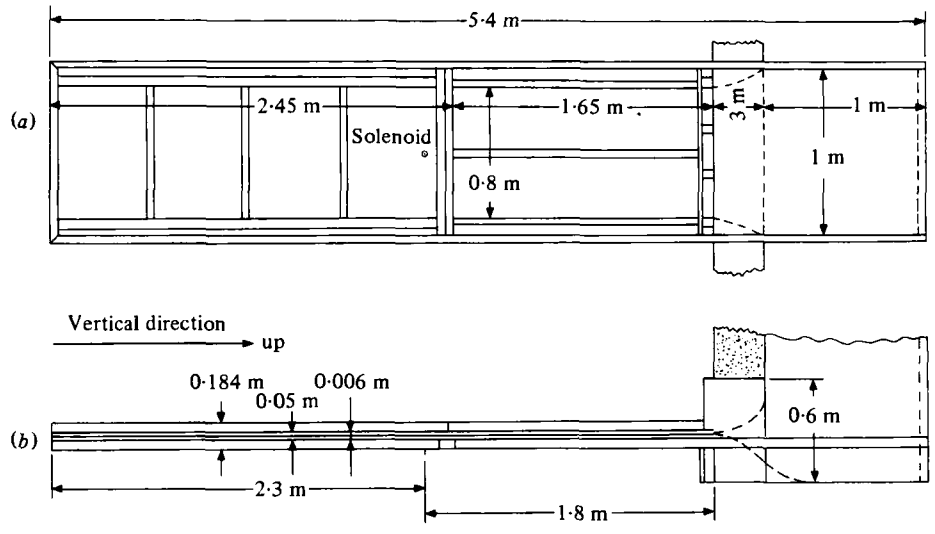

FIGURE 1. Sketch of the flow channel: (*a*) front view; (*b*) side view.

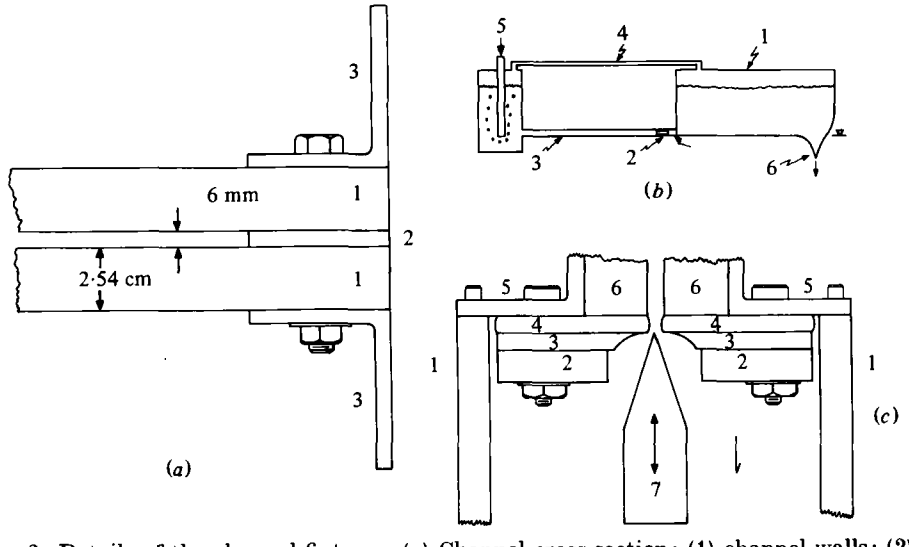

FIGURE 2. Details of the channel fixtures. (*a*) Channel cross-section: (1) channel walls; (2) side walls; (3) angle iron. (*b*) Constant-pressure-head control: (1) sealed lid; (2) honeycomb section; (3) 8 in. diameter flexible hose; (4) 3 in. diameter flexible hose; (5) atmospheric pressure; (6) channel inlet. (*c*) Channel exit and flow-control valve: (1) splash shield; (2) support plate; (3) backing plate; (4) neoprene gasket; (5) angle iron; (6) channel wall; (7) valve.

transmission, acting through a common shaft. This combination gave extremely fine position control and the addition of a neoprene outlet gasket prevented leaks. The outlet flow entered a 2·5 m^3 sump tank where it was stored until the next experimental run.

A velocity-profile development length of 1·80 m allowed a maximum test Reynolds number of approximately 5000 (assuming a top-hat velocity profile at the channel inlet; cf. Schlichting 1968). The channel had a run time given by $r_{\text{run}} = 3 \times 10^4 \text{ min}/R$ for $R = \frac{1}{2}hU_{\text{cl}}/\nu$, and $\nu = 1{\cdot}01 \times 10^{-6}$ m^2/s.

Undesirably large deflections of the channel walls would have occurred under the large static pressure load in the channel, unless special care was taken in the design of the channel, since for a given thickness a Plexiglas plate has a much smaller bending stiffness than, for example, a steel plate. Bending stiffness is $D = Eh^3/12(1-\nu_P^2)$, where E is the modulus of elasticity and ν_P is Poisson's ratio; for Plexiglas, $E = 0{\cdot}34 \times 10^{10}\,\mathrm{N/m^2}$, $\nu_P = 0{\cdot}45$. Using the Rayleigh–Ritz method to calculate the deflection of the channel walls, supported only at the side edges, under the known hydrostatic pressure loading, gave a maximum deflection at the channel exit of 0·96 cm. To reduce this unacceptable deflection, cross-braces were placed at intervals of 0·6 m along the channel, forming four test bays within which photographs could be taken. This resulted in a predicted maximum channel deflection of 0·7 mm for the lowermost part of the channel and 0·3 mm in the first bay below the solenoid.

While further reductions in channel deflection could be obtained by additional bracing, for these initial studies the $O(1$ mm) value was accepted as a reasonable compromise. Removing the braces, thus creating additional deflection, did not seem to affect the qualitative results obtained (for example the transition spots still maintained their arrowhead shape; see § 3). Also, additional bracing would have interfered with the ability to visualize the transition phenomena. Nevertheless, these small deflections at the centre of each bay undoubtedly affected the flow; this must be kept in mind when interpreting the observations. End effects modified the flow in the lower half of the last bay. Therefore, no data were taken close to the channel outlet.

Artificial disturbances were created by an electromagnetic solenoid, located in the centre of the upper portion of the test section. The solenoid plunger never entered the channel, but instead sent a pulse of fluid out through a 0·1 mm hole into the channel. This method has been noted (Matsui 1979) to generate turbulent spots of better reproducibility than those generated by electrical discharge. The amplitude of the disturbance was adjusted by simply varying the voltage of the solenoid power supply. The solenoid was triggered by a microcomputer, which was also used to trigger a camera or stroboscope.

2.2. *Flow visualization*

There is perhaps no more conceptually simple experimental tool than flow visualization to elucidate complex physical phenomena in a flow. Since the Symposium on Flow Visualization (A.S.M.E. 1960), numerous papers and conferences have described a plethora of flow-visualization techniques. There are chemical-reaction and electrically induced tracer methods, optical methods, including fluorescent dyes excited by laser sheets, tracer-injection methods, and others. Many of these techniques have been successfully applied to experimental studies of turbulence (Kline 1978).

Most of the flow-visualization techniques that are applicable to low-speed flows suffer from a common defect: they only show where the marked fluid particles go. In the present investigation, we wanted to visualize flow phenomena that did not necessarily remain with a group of fluid particles. We also required a flow-visualization technique that could be applied to a large experimental apparatus. After several techniques were tested (streaming birefringence, aluminium flakes, and fluorescent dye) and were found to have various shortcomings, titanium-dioxide-coated mica platelets (trade name Flamenco SuperPearl) were chosen. These platelets have a specific gravity (relative to water) of 3 with a size range of 10–20 μm in diameter and

a thickness of about 3–4 μm; they were used at a concentration of 0·09 % by weight. This concentration gave effective flow visualization through the entire depth of the channel.

These disc-shaped particles align themselves along the axis of principal normal stress in the flow field. However, Brownian motion tends to disorient the particles. Thus the aligning of the particles occurs only when the principal normal stresses and strain rates are high enough to overcome the randomizing effects of thermal agitation. The propagating transition spot provides this high stress–strain rate in regions of strong vorticity, turbulence and shear waves, thus allowing effective and dramatic visualization of these flow phenomena. This method of flow visualization has been used before, in Taylor-vortex apparatus for example, but to our knowledge has never been used in such large quantities in a single experiment.

No viscometer measurements were made to insure that the resulting solution was a Newtonian fluid. However, if the working fluid is Newtonian, then a dilute suspension of compact particles is likewise Newtonian for fluid motion at scales larger than the particle size, with an effective fluid viscosity that is modified by the presence of the particles (Batchelor 1967). The effective viscosity μ_{eff} of the suspension can be estimated using Einstein's formula $\mu_{\text{eff}}/\mu = 1 + 2{\cdot}5\phi$, where ϕ denotes the effective fraction of the volume occupied by particles (taken as the surrounding sphere). For the suspension used in the present investigation $\phi = 0{\cdot}0003$, giving $\mu_{\text{eff}}/\mu = 1{\cdot}000\,75$.

2.3. *Experimental procedure*

The experiments described were carried out at the Aerophysics Laboratory of the Massachusetts Institute of Technology. To reduce background noise and vibration, experiments were conducted only when other experiments in the laboratory and their associated equipment were not in use. The lower tank was filled with ordinary tap water that had been passed through a 5 μm filter. Then, 2·25 kg of titanium-dioxide-coated mica particles were added and mixed thoroughly.

Prior to an experimental run, the lower tank had to be agitated to disperse the settled tracer particles. The resulting solution was then pumped into the upper tank and allowed to sit for one or two hours to quiet the flow. An experimental run was begun by opening the valve at the channel exit to establish the flow.

Mean-velocity measurements were obtained indirectly in two different ways: first, the displacement of the free-water surface in the lower tank *vs.* time was measured and used to calculate velocity assuming Poiseuille flow; secondly, the pressure between two holes tapped four feet apart on the channel side wall was measured with a differential manometer. The resulting pressure drop was used to obtain the velocity, assuming Poiseuille flow between these points. These pressure measurements were difficult in that Δp was small compared with the static pressure in the channel. The slighest leak in any of the connecting manometer lines would lead to a significant error.

Both measurement techniques gave centreline velocities within 5 % agreement. More accurate measurement of the velocity will be obtained with a laser-Doppler velocimeter that is presently being adapted to the experiment.

Upon completion of a day's experiments the upper tank was cleaned and dried; a small fan then circulated air through the channel. This prevented hygroscopic warpage of the Plexiglas walls. Periodic cleaning of the inner channel was necessary, owing to build-up of caked tracer particles.

3. Results and objectives

The objectives of the present investigation were to obtain visual observations and some preliminary quantitative data on the transition process in plane Poiseuille flow. Since the present observations of turbulent spots in plane Poiseuille flow are without precedent, it is impossible to make detailed comparisons to other Poiseuille-flow investigations. However, some comparisons will be made with experimental observations of turbulent spots in boundary layers, where there are both striking similarities and differences.

One of the fundamental differences between turbulent spots in Poiseuille flow and in boundary-layer flow is that the spot in a channel flow remains at constant Reynolds number, whereas the spot in a normal boundary layer moves into regions of increasing Reynolds number and ultimately into turbulent flow. We were thus able to study the development of a spot that remained at constant Reynolds number, with a laminar background flow, for several hundred channel depths downstream.

3.1. *Spot structure*

Turbulent spots in plane Poiseuille flow were found to have an arrowhead shape, with a spreading half-angle of 8°, and with streamwise streaky structures trailing from the rear of the spot. Within the spot, turbulent eddies occurred which were preceded by oblique waves. Additional oblique waves were noted at the rear spanwise tips of the spot (see figure 3 for the nomenclature of a spot).

Figures 4–6 and 8 show photographs of turbulent spots located at several distances downstream of the generator: at $x/h = 50, 64, 132, 260$. The measuring tape in these photos indicates the distance from the generator in inches. Figure 7 shows a spot slightly downstream of that of figure 6; it has a number of interesting features that were not captured in the other photographs. The Reynolds number was about 1000. Figure 9 shows a spot at the same downstream distance as figure 6, but at a Reynolds number of about 1100. These photographs were taken with stroboscopic light. We found that the greatest contrast was obtained when a single source of light, located to the side, was used. This results in uneven lighting but good contrast. Photographs taken with two light sources were quite disappointing in that they showed very little contrast.

Figure 4 shows a turbulent spot a distance $x/h = 50$ from the generator. In addition to the region of small-scale turbulence and the trailing streaks, oblique waves are visible at the sides and at the rear. Visible in this photo, and noticeable in the experiment, are nearly two-dimensional waves across the turbulent region of the spot, emerging as oblique waves at the side. These waves were not prominent features of the spot further downstream.

Figure 5 shows the spot at a distance $x/h = 64$. Strong oblique waves are visible, both upstream of the leading edge of the spot and at the spanwise tips. Figure 6 shows the turbulent spot further downstream at a distance of $x/h = 132$. Again, both the region of small-scale turbulence and the wave field are clearly visible, and the front tip is less well-defined. The centre region is filled with longitudinal streaks, whereas the strong turbulence is at the spanwise tips. Figure 7 shows the development of the spot, somewhat further downstream.

One of the most striking features of these spots are the strong oblique waves and the

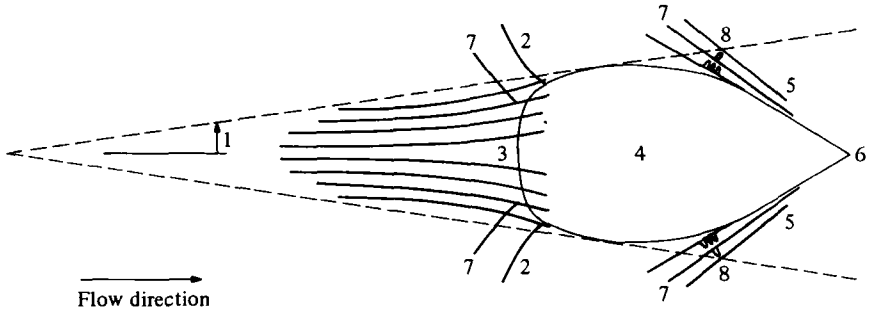

FIGURE 3. Spot nomenclature: (1) spreading half-angle; (2) spanwise tips; (3) streaks; (4) region of small-scale turbulence; (5) spot leading edge; (6) spot front; (7) oblique waves; (8) tongues of breakdown.

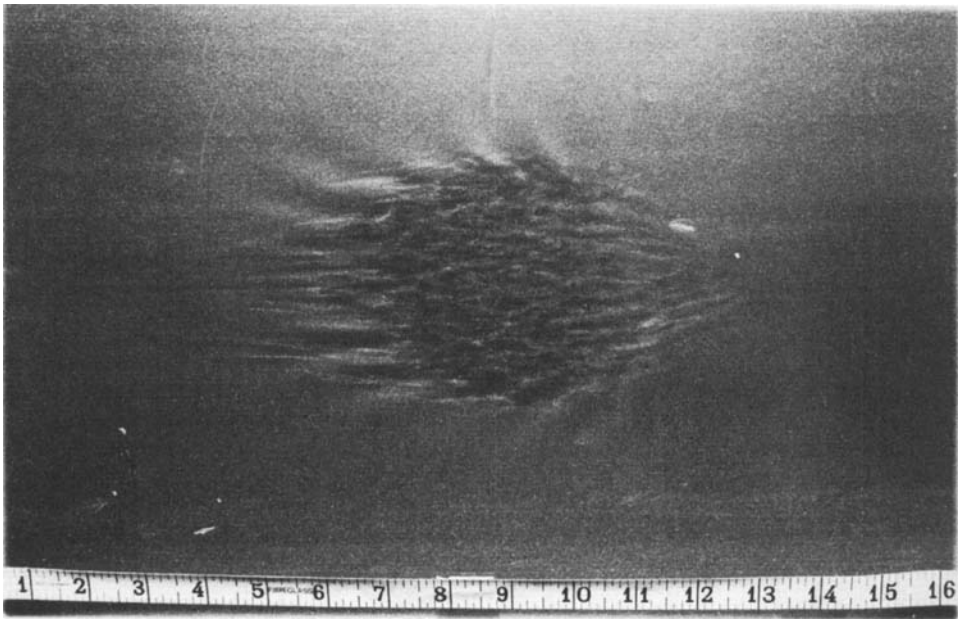

FIGURE 4. Spot at $x/h = 50$, $R = 1000$.

evident role that they play in the breakdown to turbulence. During the experiments, it was observed that, if one followed the wave crest at the leading edge of the spot, another wave appeared in front of it, suggesting that the group velocity is larger than the phase velocity. Another observation was that turbulence sprang forward in tongues of breakdown on these waves (see figure 3 for schematic). One such tongue is visible in the left of figure 7 on the second wave crest. (There is also an unexplained kink in this set of waves.) These events were quite sudden and may be related to bursting; these tongues could be related to hairpin eddy structures. Once begun, this breakdown seemed to spread in both directions along the crest.

Figure 8 shows the spot at $x/h = 260$. The spot is now quite large and very flat. Recall that the channel is 6 mm deep, while the diameter of the spot is now about 500 mm. These pictures show the important role of the waves in the breakdown to

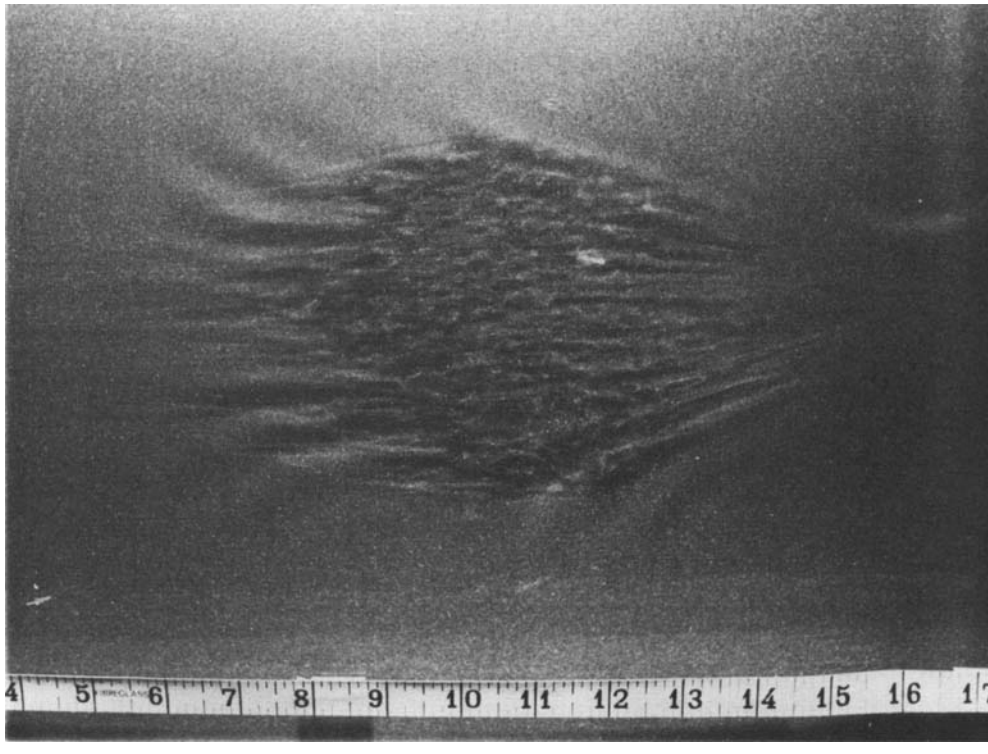

FIGURE 5. Spot at $x/h = 64$, $R = 1000$.

turbulence. The oblique waves at the outer edges of the spot proceed through the turbulent patches, refract and break, but continue through the patch and reemerge (again refracted) on the other side. Turbulence continued to appear on the new waves. The details of the shape of the spot were somewhat variable in this part of the channel but this spot is quite representative. The spot has essentially become two spots, separated by a region of longitudinal streaks. The spot on the left is beginning to develop oblique waves on its right side.

Figure 9 shows a spot at a downstream distance equal to that of figure 6, but at a higher Reynolds number. An entire sequence of photographs is available for this case and confirms the conclusions to be drawn from this picture: the oblique waves are less swept at higher R, and the wake flow is more turbulent. A more systematic study of the effects of Reynolds number will be performed in the future.

The existence of oblique wave packets in plane Poiseuille flow has not been noted before. However, Wygnanski *et al.* (1979) found, through hot-wire measurements, that oblique wave packets exist near the rear spanwise tips of a turbulent spot in a laminar boundary layer. These wave packets exhibited frequency and wave-speed characteristics of oblique Tollmien–Schlichting waves. In their boundary-layer flow-visualization experiments, Gad-el-Hak *et al.* (1979) found that a large-amplitude wavelike structure preceded the passage of a turbulent spot. These waves were thought to be oblique Tollmien–Schlichting waves. However, since they were using a tracer-particle visualization technique, they did not obtain a clear visualization of the structure of the wave field.

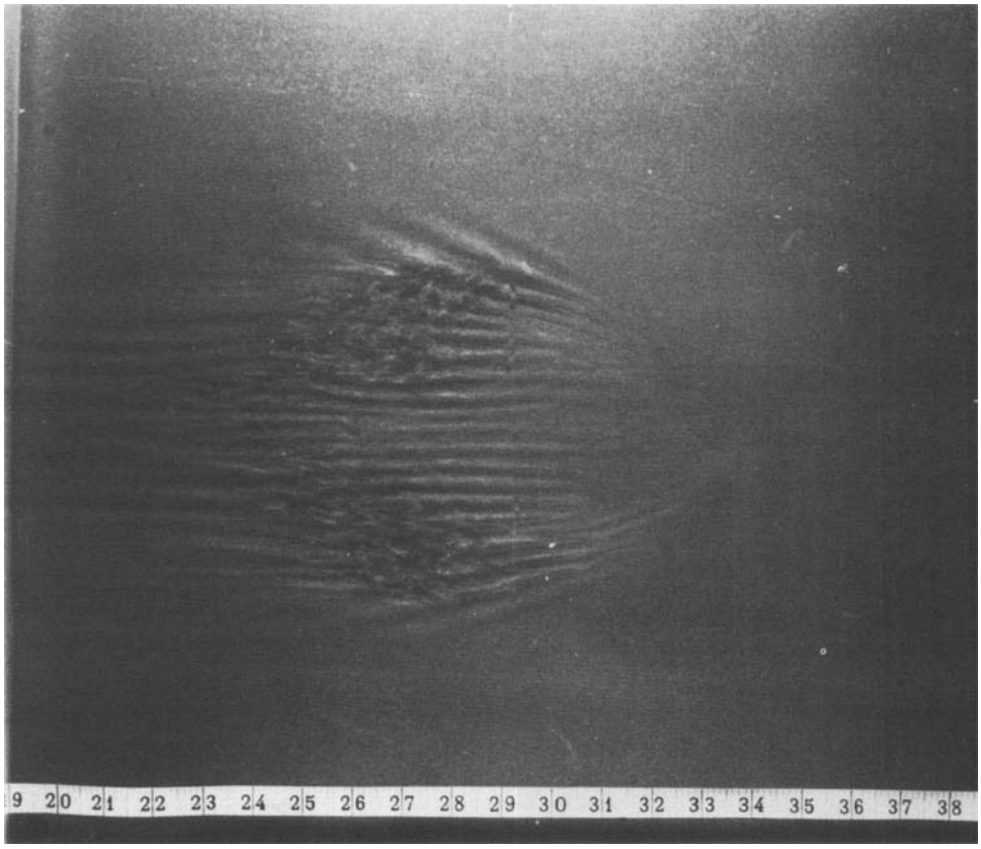

FIGURE 6. Spot at $x/h = 132$, $R = 1000$; beginning of spot splitting.

The flow-visualization study of Cantwell *et al.* (1978), of the sublayer structure of a turbulent spot in a boundary-layer flow, did not reveal any wavelike phenomena. Since they were using aluminium flakes, which behave similarly to our mica particles, they might have been expected to visualize waves. However, the extremely opaque suspension that they used gave effective visualization of only the sublayer, since the viewing depth into the flow was only about 2 mm.

Our observations of the growth of a turbulent spot in plane Poiseuille flow showed that the occurrence of transition is a function of the Reynolds number. Below a Reynolds number of about 840, a disturbance was found to grow into a semideveloped spot and then to decay into streamwise structures that ultimately disappeared. These spots decayed before strong wave disturbances were observed. Although finite-amplitude effects are thought to be important in Poiseuille flow, this decay occurred over a range of disturbance amplitudes. At a Reynolds number of about 1000, a strong, repeatable, growing spot could be triggered. This spot was not noticeably sensitive to disturbance amplitude. If the Reynolds number was raised further above 1200, natural turbulent spots appeared randomly across the span and along the length of the channel. Figure 10 shows typical natural transition at a Reynolds number of about 1200. The shape of the natural turbulent spot was very similar to that of the

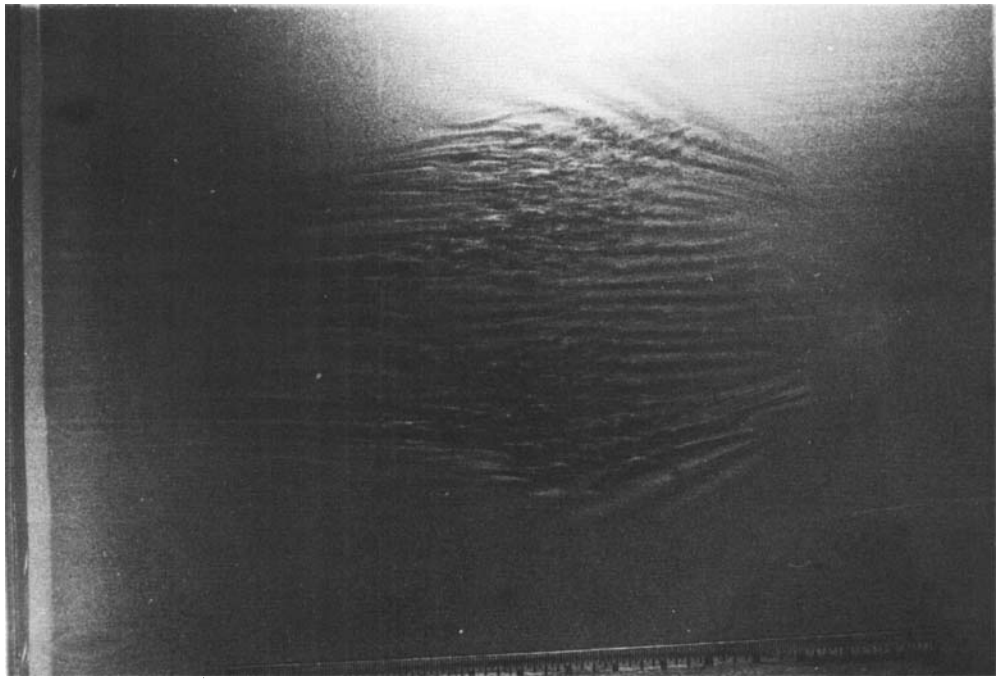

FIGURE 7. Spot downstream of $x/h = 132$ at $R = 1000$.

artificially generated spot. Further increases in the Reynolds number above about 1500 resulted in a fully turbulent flow field. We have not, as yet, done any systematic study of natural transition including the effects of background disturbances or inlet geometry.

The observed transition Reynolds number of about 1000 is consistent with what other experimental investigators have obtained. However, this value is far below what two-dimensional linear and nonlinear theories predict for the critical Reynolds number. Application of linear stability theory predicts a critical Reynolds number of over 5000 (Lin 1945*a*, *b*, *c*; Thomas 1952; Orszag 1971). Stuart (1960) carried out a nonlinear stability analysis, and obtained a subcritical transition Reynolds number of 2900. Orszag & Kells (1980), by direct numerical solution of the Navier–Stokes equations, inferred from the behaviour of the calculations a transition Reynolds number of about 1000, when finite-amplitude three-dimensional disturbances were considered. These later calculations come closest to the transition Reynolds number obtained in our experiments.

Since the present investigation is in a bounded geometry, the growth of the turbulent spot cannot be explained by arguments about entrainment (the propagation of the laminar–turbulent interface into the laminar fluid by the viscous and small-scale turbulent diffusion of vorticity) from the free stream. Entrainment also cannot explain the spanwise spreading rates obtained in our experiment. The experimental observations presented here indicated that the spanwise growth of an individual spot is related to the breakdown to turbulence in the oblique wave field at the leading edge of the spot.

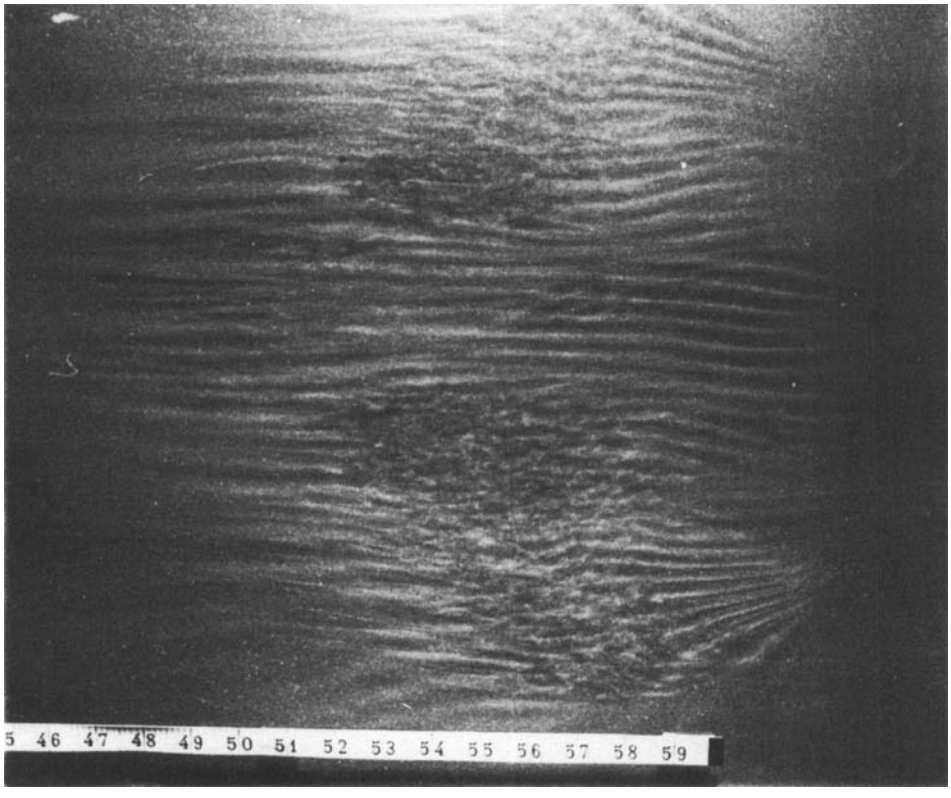

FIGURE 8. Spot at $x/h = 260$, $R = 1000$.

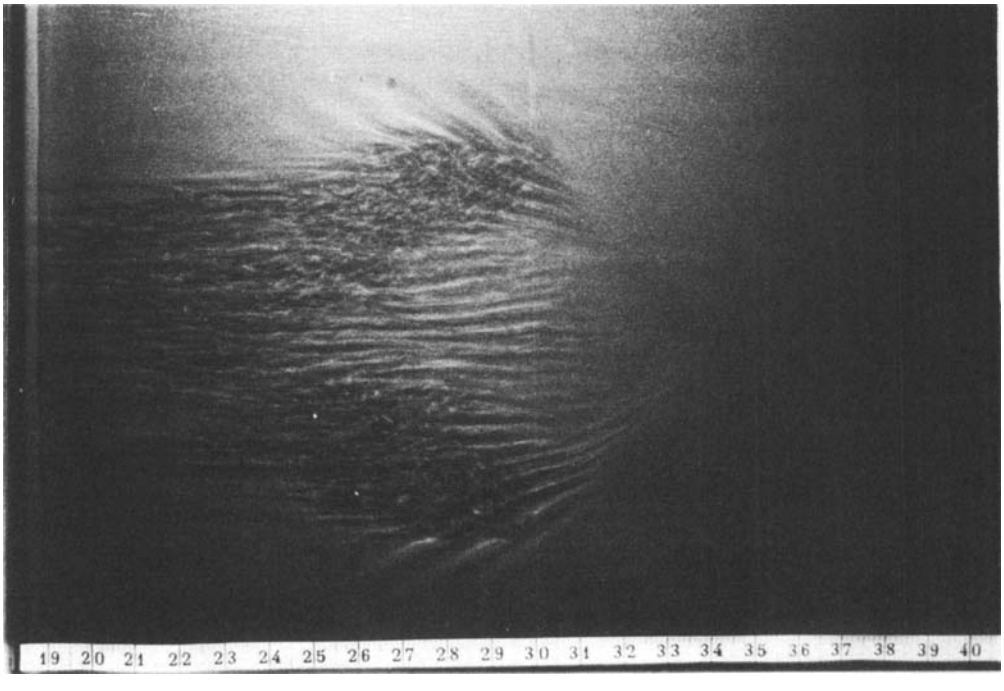

FIGURE 9. Spot at $x/h = 132$, $R = 1100$.

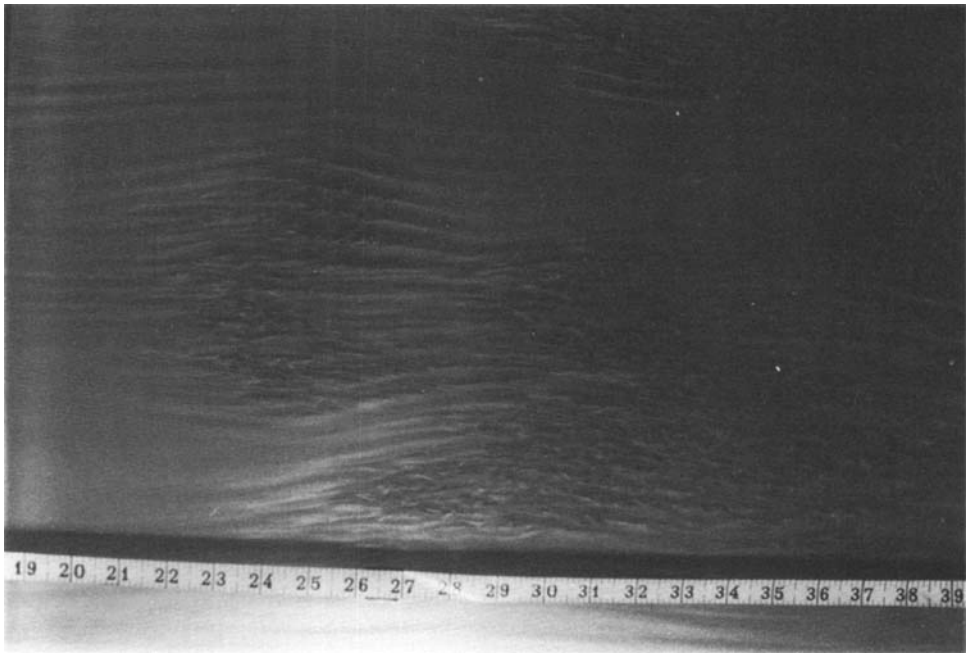

FIGURE 10. Natural transition at $R \approx 1200$.

Gad-el-Hak *et al.* (1979) suggested that turbulent eddies within a boundary-layer spot induce perturbations into the surrounding unstable fluid, resulting in local breakdown, which they termed 'growth by destabilization'. Their experiments seem to indicate the breakdown of a wavelike structure in the Blasius boundary layer just ahead of the oncoming turbulent region. The present investigation has established that oblique waves exist at the leading edge of the turbulent spot in plane Poiseuille flow, as well as at its spanwise tips, and that this local wave breakdown appears to be the dominant mechanism for the spatial growth of a turbulent spot in this flow. One remaining difficulty is that the undisturbed channel flow is stable to infinitesimal waves at these Reynolds numbers.

One of the most striking phenomena was the observed splitting of a turbulent spot, accompanied by strong wave activity, as the spot moved downstream. The initial sharply defined arrowhead shape, as shown in figure 5, grew rapidly and metamorphosed as it travelled downstream.

The sequence of photographs of figures 4–8 show the natural development of the splitting of the spot. The spot of figure 6 at $x/h = 132$ has begun to round off, and what appears to be a calmed region is beginning to appear at the centre of the spot's front. This becomes more pronounced in figure 7. Figure 8 shows a spot that was 1·65 m from the initial disturbance. Splitting is nearly complete, and the centre is free of small-scale turbulence. Just before the spot left the channel, two distinct spots had formed. No pictures of this are included, since end effects clearly distorted the spots.

Splitting of coherent structures in pipe flow has been observed by Rubin, Wygnanski & Haritonidis (1979), but to our knowledge has not been reported in boundary-layer

flow. Why this pronounced splitting occurs in Poiseuille flow and (apparently) not in boundary layers is unclear.

A possible explanation for the observed splitting of the spot arises when one compares the energy-transfer mechanism for channel and boundary-layer flows. Turbulent spots in a boundary layer entrain irrotational fluid from the free stream, feeding energy into the spot's centre region. However, because of the bounded geometry, there can be no large-scale entrainment of fluid into the centre region of a spot in plane Poiseuille flow. This lack of energy transfer to the spot's centre results in relaminarization within the spot through the action of viscosity.

Although the spot was produced by an asymmetric disturbance at one wall, it was observed, in photographs taken from the backside of the test section, to fill the depth of the channel within a few channel widths from the generator. In addition, the turbulent spot maintained its arrowhead shape even if the background flow was moderately turbulent. This turbulent background flow, primarily in the form of longitudinal vorticity, occurred whenever the channel was run in a recirculating mode, resulting in flow disturbances in the upper tank. This coherence of spot shape, in spite of the existence of a turbulent background flow, was also noted by Zilberman, Wygnanski & Kaplan (1977). They found that spots survived buffeting by the surrounding turbulence in a turbulent boundary layer.

3.2. *Propagation velocity measurements*

The propagation velocities of the front and rear of a turbulent spot in plane Poiseuille flow were measured from videotaped records of the spot. Figure 11 shows the measured position of the front and rear of the spot *vs.* time at a Reynolds number of 1000. Because the front point of the spot was not always distinct, it was somewhat difficult to define its position. We used the projections of the oblique waves to define the spot front. However, with proper lighting there exists an identifiable front tip to the spot visible in the photographs at the forward extension of the waves.

Data taken from video-camera positions located in bays 1 and 2 are given in figure 11. The time axis is relative: zero does not correspond to the trigger, and the data from the two camera positions was fitted together to make a smooth curve for the position of the front point. This data indicates that the front of the spot has a propagation velocity of 19 cm/s while the rear moves at 11 cm/s. The centreline velocity U_{cl} of the background Poiseuille flow was estimated from volume-flow measurements to be 32 cm/s. Thus the front of the spot moves with a propagation velocity of about $0{\cdot}6U_{\mathrm{cl}}$, while the rear moves at a propagation velocity of $0{\cdot}34U_{\mathrm{cl}}$.

In the present set of experiments, no strong dependence of these normalized propagation velocities on Reynolds number was obtained. When the LDV is installed to allow an accurate on-line measurement of centreline velocity, this question will be investigated further.

There is some theoretical significance to the fact that the front tip of the spot moves with a propagation velocity slightly below $\frac{2}{3}U_{\mathrm{cl}}$. It was Gustavsson who first point out that there could be a connection between the continuous spectrum of the Orr–Sommerfeld equation, which propagates at the free-stream speed, and the fact that the non-dimensional propagation velocity of the point of a turbulent spot in a boundary layer is just below 1·0. In considering the initial-value problem for a Blasius boundary layer, Gustavsson (1979) showed that disturbances described by the con-

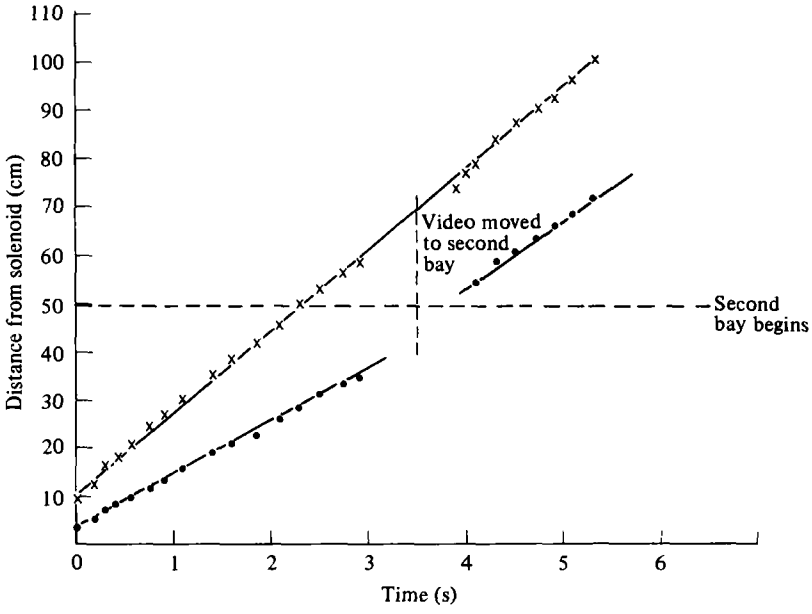

FIGURE 11. Position of the leading and trailing edges of the spot at $R = 1000$, $U_{cl} = 32$ cm/s.

tinuous spectrum move with the free-stream velocity throughout the boundary layer. Gustavsson speculated that the arrowhead shape of a turbulent spot in a boundary layer could be attributed to the interaction between the high speed of the continuous spectrum and the least damped Tollmien–Schlichting wave.

While a continuous spectrum does not exist for plane Poiseuille flow, the recent calculations of Gustavsson (1981) show a cluster of eigenmodes around $c_r = \frac{2}{3}$. This cluster of modes may play a role in determining the shape of the spot analogous to that played by the continuous spectrum in the boundary layer. Thus for Poiseuille flow the propagation of the tip of the spot at a non-dimensional propagation velocity just below $\frac{2}{3}$ may be analogous to the propagation of the front tip of the spot in a boundary layer at a value just below 1·0. Although not conclusive, this suggests that the value $U_{front}/U_{cl} = \frac{2}{3}$, for a spot in Poiseuille flow, may be related to this cluster of eigenmodes.

3.3. *Concluding remarks*

The titanium-dioxide-coated mica particles were very effective in revealing the structure of a turbulent spot in plane Poiseuille flow. Rather than providing visualization of dyed particles, this technique provided a more dynamic visualization of disturbances, including those that propagate through the fluid and form regions of strong shear waves, vorticity and breakdown to turbulence. The spot was characterized by the appearance of oblique wave packets surrounding an arrowhead-shaped coherent structure. Some preliminary measurements of the relative propagation velocities were made and compared with recent theoretical work. In addition, turbulent spots were found to split and form two new spots.

This experiment afforded a very dramatic view of strong wave structures preceding,

passing through and trailing turbulent spots. At Reynolds numbers far below critical, these waves are linearly damped, and yet their breakdown sustains the turbulent spot, which in turn generates new laminar waves. Few theoretical explanations of such strong subcritical wave generation are available. We have looked at the algebraic growth mechanism of Gustavsson (1981), which contains some predictions about what oblique waves might be resonant at our test conditions. From the wavenumber results that he presented, we calculated the angle of oblique waves that would be resonant at $R = 1000$. The most-amplified wave had an angle of 19°; other waves were predicted at 36° and 63°. In the experiment, the angle of the leading-edge waves varied from about 18° (figure 6) to 25° (figure 7) and, at higher Reynolds number, 37°. This agreement in wave angle must be tempered by the observation that the agreement in wavelength and wave speed was not as good. The relation between our experimental results and the oblique wave resonance of Gustavsson therefore remains unclear. However, we plan to pursue these ideas and to investigate the calculation of wave-packet phenomena in Poiseuille flow below R_c.

This research was sponsored by the AFOSR under contract number AFOSR-81-0031; Captain M. Francis was the contract monitor. We acknowledge the active participation of many colleagues including L. H. Gustavsson, Marten Landahl, Willem Malkus and Sinan Ackmandor.

REFERENCES

A.S.M.E. 1960 *Symp. on Flow Visualization.* A.S.M.E.

Batchelor, G. K. 1967 *An Introduction to Fluid Mechanics.* Cambridge University Press.

Cantwell, B. J. 1981 Organized motion in turbulent flow. *Ann. Rev. Fluid Mech.* **13**, 457–515.

Cantwell, B., Coles, D. & Dimotakis, P. 1978 Structure and entrainment in the plane of symmetry of a turbulent spot. *J. Fluid Mech.* **87**, 641–672.

Elder, J. W. 1960 An experimental investigation of turbulent spots and breakdown to turbulence. *J. Fluid Mech.* **9**, 235–246.

Emmons, H. W. 1951 The laminar–turbulent transition in a boundary layer – Part I. *J. Aero. Sci.* **18**, 490–498.

Gad-el-Hak, M., Blackwelder, R. F. & Riley, J. J. 1979 A visual study of the growth and entrainment of turbulent spots. In *Laminar–Turbulent Transition* (ed. R. Eppler & H. Fasel), pp. 297–310. Springer.

Grosch, C. E. & Salwen, H. 1978 The continuous spectrum of the Orr–Sommerfeld equation. Part 1. The spectrum and the eigenfunctions. *J. Fluid Mech.* **87**, 33–54.

Gustavsson, L. H. 1978 On the evolution of disturbances in boundary layer flows. *Tech. Rep.* TRITA-MEK-78-02, *Dept of Mechanics, KTH, Stockholm.*

Gustavsson, L. H. 1979 Initial-value problem for boundary layer flows. *Phys. Fluids* **22**, 1602–1605.

Gustavsson, L. H. 1981 Resonant growth of three-dimensional disturbances in plane Poiseuille flow. *J. Fluid Mech.* **112**, 253–264.

Gustavsson, L. H. & Hultgren, L. 1980 A resonance mechanism in plane Couette flow. *J. Fluid Mech.* **98**, 149–159.

Kao, T. W. & Park, C. 1970 Experimental investigations of the stability of channel flows. Part 1. Flow of a single liquid in a rectangular channel. *J. Fluid Mech.* **43**, 145–164.

Karnitz, M. A., Potter, M. C. & Smith, M. C. 1974 An experimental investigation of transition of a plane Poiseuille flow. *Trans. A.S.M.E.* I, *J. Fluids Engng* **96**, 384–388.

Kline, S. J. 1978 The role of visualization in the study of the structure of the turbulent boundary layer. In *Proc. Lehigh Workshop on Coherent Structures of Turbulent Boundary Layers*, pp. 1–26.

LIN, C. C. 1945*a* On the stability of two-dimensional parallel flows. Part I. General theory. *Q. Appl. Math.* **3**, 117–142.

LIN, C. C. 1945*b* On the stability of two-dimensional parallel flows. Part II. Stability in an inviscid fluid. *Q. Appl. Math.* **3**, 218–234.

LIN, C. C. 1945*c* On the stability of two-dimensional parallel flows. Part III. Stability in a viscous fluid. *Q. Appl. Math.* **30**, 277–301.

MACK, L. M. 1967 A numerical study of the temporal eigenvalue spectrum of the Blasius boundary layer. *J. Fluid Mech.* **73**, 497–520.

MATSUI, T. 1979 Visualization of turbulent spots in the boundary layer along a flat plate in a water flow. In *Laminar–Turbulent Transition* (ed. R. Eppler & H. Fasel), pp. 288–296. Springer.

MITCHNER, M. 1954 Propagation of turbulence from an instantaneous point disturbance. *J. Aero. Sci.* **21**, 350–351.

NARAYANAN, M. A. B. & NARAYANA, T. 1967 Some studies on transition from laminar to turbulent flow in a two-dimensional channel. *Z. angew. Math. Mech.* **18**, 642–650.

NISHIOKA, M., IIDA, S. & ICHIKAWA, Y. 1975 An experimental investigation of the stability of plane Poiseuille flow. *J. Fluid Mech.* **72**, 731–751.

NISHIOKA, M., ASAI, M. & IIDA, S. 1980 Wall phenomena in the final stage of transition to turbulence. In *Transition and Turbulence* (ed. R. E. Mayer). Academic.

ORSZAG, S. A. 1971 Accurate solutions of the Orr–Sommerfeld stability equation. *J. Fluid Mech.* **50**, 689–703.

ORSZAG, S. A. & KELLS, L. C. 1980 Transition to turbulence in plane Poiseuille flow and plane Couette flow. *J. Fluid Mech.* **96**, 159–205.

ORSZAG, S. A. & PATERA, A. T. 1980 Subcritical transition to turbulence in plane channel flows. *Phys. Rev. Lett.* **45**, 989–993.

PATEL, V. C. & HEAD, M. R. 1969 Some observations on skin friction and velocity profiles in fully developed pipe and channel flows. *J. Fluid Mech.* **38**, 181–201.

RUBIN, Y., WYGNANSKI, I. & HARITONIDIS, J. H. 1979 Further observations on transition in a pipe. In *Laminar–Turbulent Transition* (ed. R. Eppler & H. Fasel), pp. 288–296. Springer.

SCHLICHTING, H. 1968 *Boundary Layer Theory*, 6th edn, p. 177. McGraw-Hill.

SCHUBAUER, G. B. & KLEBANOFF, P. S. 1956 Contributions on the mechanics of boundary layer transition. *NACA Rep.* no. 128.

SCHUBAUER, G. B. & SKRAMSTAD, H. K. 1948 Laminar boundary layer oscillations on a flat plate. *NACA Rep.* no. 909.

SHERLIN, G. C. 1960 Behavior of isolated disturbances superimposed on laminar flow in a rectangular pipe. *J. Res. Nat. Bur. Stand.* **64A**, 281–289.

STUART, J. T. 1960 On the non-linear mechanics of wave disturbances in stable and unstable parallel flows. *J. Fluid Mech.* **9**, 353–370.

THOMAS, L. H. 1952 The stability of plane Poiseuille flow. *Phys. Rev.* **86**, 812–813.

WYGNANSKI, I., HARITONIDIS, J. H. & KAPLAN, R. E. 1979 On a Tollmien–Schlichting wave packet produced by a turbulent spot. *J. Fluid Mech.* **92**, 505–528.

WYGNANSKI, I., SOKOLOV, M. & FRIEDMAN, D. 1976 On a turbulent 'spot' in a laminar boundary layer. *J. Fluid Mech.* **78**, 785–819.

ZILBERMAN, M., WYGNANSKI, I. & KAPLAN, R. E. 1977 Transitional boundary layer spot in a fully turbulent environment. *Phys. Fluids* **20**, 258–271.